




# Developing Novel Robust Models to Improve the Accuracy of Daily Streamflow Modeling

Babak Mohammadi<sup>1</sup> · Farshad Ahmadi<sup>2</sup> · Saeid Mehdizadeh<sup>3</sup> · Yiqing Guan<sup>1</sup> · Quoc Bao Pham<sup>4,5</sup> · Nguyen Thi Thuy Linh<sup>6</sup> · Doan Quang Tri<sup>7</sup> 

Received: 2 February 2020 / Accepted: 2 July 2020 /

Published online: 13 July 2020

© Springer Nature B.V. 2020

## Abstract

Streamflow plays a major role in the optimal management and allocation of available water resources in each region. Reliable techniques are therefore needed to be developed for streamflow modeling. In the present study, the performance of streamflow modeling is improved via developing novel boosted models. The daily streamflows of four hydrometric stations comprising of the Brantford and Galt stations located on the Grand River, Canada, as well as Macon and Elkton stations respectively, located on the Ocmulgee and Umpqua rivers, United States, are used. Three different types of boosted models are implemented and proposed by coupling the classical multi-layer perceptron (MLP) with the optimization algorithms, including particle swarm optimization (PSO) and coupled particle swarm optimization-multi-verse optimizer (PSOMVO) and a time series model, namely the bi-linear (BL). So, the boosted MLP-PSO, MLP-PSOMVO, and MLP-BL models are developed. The accuracy of all the boosted models is compared with the classical MLP and BL by the statistical metrics used. It is concluded that all the boosted models developed at the studied stations lead to superior modeling results of the daily streamflows to the classical MLP; however, the boosted MLP-BL models generally outperformed the MLP-PSO and MLP-PSOMVO ones.

**Keywords** Daily streamflow · Multi-layer perceptron · Particle swarm optimization · Multi-verse optimizer · Bi-linear

## 1 Introduction

Streamflow is an essential component of the water cycle. It can give significant information to design water infrastructures and flood control systems, to mitigate the impacts of droughts on available water resources systems, to optimize management of the irrigation and agriculture at

---

✉ Doan Quang Tri  
doanquangtri@tdtu.edu.vn

any particular region, to generate hydropower, etc. (Yaseen et al. 2016; Anghileri et al. 2016; Tikhamarine et al. 2019a; Fang et al. 2019). Therefore, knowing the streamflow time series is a necessity for hydrologists, water resources managers, and decision-makers. Streamflow is expected to include the non-linear, stochastic, and non-stationary behaviors that make a complex phenomenon (Bayazit 2015). Given this, robust techniques are required to be used and developed by the hydrologists to capture the features as mentioned above.

In a general classification, streamflow modeling approaches can be categorized in main two groups, including the physically-based techniques and the data-driven models (Peugeot et al. 2003; He et al. 2014; Di et al. 2014; Zhang et al. 2016). The streamflow time series are simulated in the physically-based models through modeling the potential interactions among the various factors consisting of the weather information, land surface characteristics, etc. (Wang et al. 2016; Fang et al. 2019). These models, therefore, seem to be complicated to use in the applications. Furthermore, the data-driven models are another type of streamflow modeling techniques. They have the capability to model the streamflow process via historical records of streamflow or other variables without any need to know the physical procedures governing the streamflow process (Di et al. 2014; Garcia et al. 2016; Zhang et al. 2016). Two well-known and commonly used types of data-driven models in streamflow forecasting are the time series models and artificial intelligence (AI) techniques. However, the application of AI techniques has received a widespread interest; while the time series models have been used lesser than the AI ones in streamflow modeling.

It is proven that the standalone classical models couldn't provide appropriate performances for modeling the hydrological time series (e.g., streamflow). Therefore, major efforts have been made to improve the modeling accuracy of the standalone models. Recently, implementing boosted models has received remarkable progress by many researchers. In this context, coupling the standalone models such as AI-based approaches with the wavelet analysis, the time series models, the optimization algorithms, etc. can be taken into consideration as alternatives to the standalone models with a reliable level of performance. The boosted models generated via integrating the AI and time series models could demonstrate higher accuracies since both the outputs of the models as mentioned above are considered through a boosted AI-time series model. In fact, the standalone classical AI and time series models focus only on the modeling/capturing the deterministic and stochastic segments, respectively, while the boosted models use both terms to improve the modeling performance. Furthermore, the optimization algorithms are coupled with the AI models in order to find the minimum cost of the AI function and to improve training phase of the AI models. Recently, the practice of metaheuristic optimization algorithms demonstrated a considerable potential solution to alleviate the difficulties exist with training and parameterization of AI models. These algorithms enable automatically learner of the AI models and improve the model performance (Pham et al. 2020; Mohammadi 2019a, 2019b; Moazen-zadeh et al. 2018). Various bio-inspired meta-heuristic algorithms have been invented to cope with optimization issues by imitation of the hydrological phenomena. Some of those prevalent nature-inspired meta-heuristic algorithms includes shuffled frog leaping algorithm (Mohammadi et al. 2020), particle swarm optimization (Tikhamarine et al. 2019b), bee colony algorithm (Choong et al. 2017), genetic algorithm (Jahani and Mohammadi 2019), krill-herd algorithm (Moazen-zadeh and Mohammadi 2019,

Mohammadi and Aghashariatmadri 2020), gray wolf optimizer algorithm (Maroufpoor et al. 2020; Tikhamarine et al. 2019a), firefly algorithm (Aghelpour et al. 2019), whale optimization algorithm (Mohammadi and Mehdizadeh 2020; Vaheddoost et al. 2020), and particle swarm optimization (Aghelpour et al. 2020).

In recent years, the application of AI-based models has received significant attention in modeling the streamflow time series on various time scales including the daily and monthly. Some of detailed information of previous works reviewed in this study is summarized (Table 1).

As can be concluded from the literature review mentioned in Table 1, the time series models have received less attention in streamflow modeling. In addition, the boosted models have illustrated superior performances compared to the standalone models that confirms the need to develop boosted models to precisely modeling of streamflow time series.

The chief purpose of this research work is to enhance the modeling accuracy of daily streamflow time series at two hydrometric stations in Canada, and two others in United States. In this process, an AI-based model including the multi-layer perceptron (MLP) is coupled with the particle swarm optimization (PSO), particle swarm optimization coupled on multi-verse optimizer (PSOMVO), and bi-linear (BL) models. Besides developing the aforementioned boosted models, the performance of classical MLP and BL is also evaluated in modeling the daily streamflows and then compared to the boosted models proposed. The innovative aspects of this study are to develop the boosted MLP-PSOMVO and MLP-BL, as well as the classical BL time series model. To the best of authors' knowledge, this study is the first attempt in literature for the daily streamflow modeling through the boosted MLP-BL and MLP-PSOMVO models. Main reason to select the non-linear BL model is that it includes the potential for capturing the stochastic term of streamflow as a non-linear phenomenon in hydrologic cycle. Additionally, according to literature and reviews MLP model has good performance for predicting streamflow. And nature-inspired optimization such as PSO and MVO algorithm can be improved ability of classic MLP, then MLP-PSOMVO can be a proposed model for predicting streamflow by high accuracy in compression classic MLP model.

## 2 Materials and Methods

### 2.1 Study Area and Data Used Description

To carry out this research work, the daily streamflow information of two hydrometric stations in the Canada and two other ones in the United States are used. The Brantford and Galt stations located on the Grand River in Canada are considered. The Grand River with a length of 280 km is one of the large rivers in southwestern Ontario. It is completely within the boundaries of southern Ontario. Furthermore, the Macon station located on Ocmulgee River and near Elkton station located on Umpqua River, United States, are selected. The Macon and Elkton stations are respectively located in Georgia State of the southeastern United States and Oregon State of the northwestern United States. The geographical information of studied hydrometric stations and statistical properties of the observed daily streamflows including the minimum ( $X_{\min}$ ), maximum ( $X_{\max}$ ), mean ( $X_{\text{mean}}$ ), standard deviation ( $X_{\text{sd}}$ ), and coefficient of variation ( $X_{\text{cv}}$ ) for

**Table 1** Information of previous studies published in literature reviewed in the current study

Reference	Case study	Time scale	Models used	Best model
Abudu et al. (2010)	Kizil River, China	Monthly	ANN, ARIMA, SARIMA	Similar results were reported
Adamowski et al. (2012)	mountainous watershed of Sainji in the Himalayas	Daily	MARS, ANN, W-ANN	MARS, W-ANN
Kisi et al. (2012)	Ergene River and Seytan Stream, Turkey	Daily	ANN, ANFIS, SVM, LLR, DLLR	ANN, ANFIS
Liu et al. (2014)	Fork White River and Eel River, USA	Daily and monthly	SVR, W-SVR	W-SVR
Uysal et al. (2016)	Karasu River, Turkey	Daily	MLP, RBFNN	MLP
Abdollahi et al. (2017)	Behesht-Abad and Joneghan rivers, Iran	Daily	ANN, GEP, W-ANN, W-GEP	W-ANN
Siqueira et al. (2018)	Brazilian hydroelectric plants	Monthly	ELM, ESN, MLP, PAR	ESN
Hadi and Tombul (2018)	Goksu-Gokdere Basin, Turkey	Monthly	ANN, MGGP, W-ANN, W-MGGP	MGGP
Tongal and Booij (2018)	North Fork, Chehalis, Carson and Sacramento rivers	Daily	ANN, SVM, RF	ANN, RF
Al-Sudani et al. (2019)	Tigris River, Iraq	Monthly	MARS, LSSVR, MARS-DE	MARS-DE
Mehdizadeh et al. (2019a)	Sefidrood River, Iran and Saugeen River, Canada	Monthly	AR, MA, AR-ARCH, MA-ARCH, MARS, GEP	MARS and GEP under external analysis
Mehdizadeh et al. (2019b)	Ocmulgee and Umpqua rivers, USA	Monthly	MARS, GEP, MLR, MARS-FARIMA, MARS-SETAR, GEP-FARIMA, GEP-SETAR, MLR-FARIMA, MLR-SETAR	MLR-FARIMA and MLR-SETAR
Fathian et al. (2019)	Grand River, Canada	Monthly	ANN, MARS, RF, ANN-SETAR, ANN-GARCH, MARS-SETAR, MARS-GARCH, RF-SETAR, RF-GARCH	MARS-SETAR
Tikhmarine et al. (2019a)	Aswan High Dam, Iraq	Monthly	ANN, SVR, MLR, ANN-GWO, SVR-GWO, MLR-GWO	SVR-GWO

ANN: artificial neural networks, ARIMA: autoregressive integrated moving average, SARIMA: seasonal ARIMA, MARS: multivariate adaptive regression splines, W-ANN: wavelet-artificial neural networks, ANFIS: adaptive neuro-fuzzy inference system, SVM: support vector regression, LLR: local linear regression, DLLR: dynamic local linear regression, SVR: support vector regression, W-SVR: wavelet-support vector regression, MLP: multi-layer perceptron, RBFNN: radial basis function neural network, GEP: gene expression programming, W-GEP: wavelet-gene expression programming, ELM: extreme leaning machine, ESN: echo state network, PAR: partial autoregressive, MGGP: multigene genetic programming, W-MGGP: wavelet-multigene genetic programming, RF: random forests, LSSVR: least square support vector regression, MARS-DE: multivariate adaptive regression splines-differential evolution, AR: autoregressive, MA: moving average, ARCH: autoregressive conditional heteroscedasticity, MLR: multiple linear regression, FARIMA: fractionally ARIMA, SETAR: self-exciting threshold autoregressive, GARCH: generalized ARCH, GWO: gray wolf optimization

both the train and test phases are presented (Table 2). The geographical locations of the studied hydrometric stations in the Canada and United States are depicted (Fig. 1).

The daily streamflow time series of the studied sites span the water years from 1 Oct. 1998 to 30 Sep. 2018 (i.e., 20-year). The daily streamflow data of the Canadian and American stations are acquired from (<https://wateroffice.ec.gc.ca>) and (<http://water>.

**Table 2** Statistical parameters of the observed daily streamflow data for the studied sites during train and test phases

Stations	River	Longitude (°W)	Latitude (°N)	Phases	X <sub>min</sub>	X <sub>max</sub>	X <sub>mean</sub>	X <sub>sd</sub>	X <sub>cv</sub>
Brantford	Grand	80.27	43.12	Train	8.000	1000.000	60.260	69.998	1.162
				Test	16.400	728.000	69.036	76.070	1.102
Galt	Grand	80.30	43.35	Train	5.190	549.000	41.431	50.597	1.221
				Test	6.450	780.000	46.093	58.627	1.272
Macon	Ocmulgee	83.62	32.83	Train	5.748	957.115	61.967	84.503	1.364
				Test	6.060	1449.830	71.540	111.773	1.562
Elkton	Umpqua	123.55	43.58	Train	24.324	4247.550	195.569	270.832	1.385
				Test	21.917	3143.187	195.742	288.197	1.472

[usgs.gov/waterwatch/](https://usgs.gov/waterwatch/)), respectively. In this study, whole the data are split into the train (i.e., 75% of the data between 1 Oct. 1998 and 30 Sep. 2013) and test (i.e., 25% of the data between 1 Oct. 2013 and 30 Sep. 2018) datasets (Fig. 2). As clearly can be seen in Table 2, the statistical parameters of the daily streamflows at the studied locations are almost the same for the train and test stages.

The following equation is used in this study to standardize the observed daily streamflows of the studied sites as:

$$Q_s = \frac{Q_o - \overline{Q_o}}{\sigma_{Q_o}} \tag{1}$$

where  $Q_s$  illustrates the standardized daily streamflow,  $Q_o$  is the observed daily streamflow,  $\overline{Q_o}$  represents the mean of observed daily streamflows for each train and test periods, and  $\sigma_{Q_o}$  denotes the standard deviation of the observed daily streamflows for each train and test phases.

### 2.2 Bi-Linear (BL) Time Series Model

Non-linear BL model was initially proposed by Granger and Andersen (1978). It is developed based on the ARMA models. The BL model is extracted from the second-order extension of Taylor series and displayed as  $BL(p, q, r, s)$  (Fan and Yao 2003). It can be formulated as the following equation:

$$Z_t = \sum_{i=1}^p (\varphi_i \cdot Z_{t-i}) - \sum_{j=1}^q (\theta_j \cdot \varepsilon_{t-j}) + \sum_{i=0}^r \sum_{j=1}^s (\beta_{ij} \cdot Z_{t-i-j} \cdot \varepsilon_{t-j}) + \varepsilon_t \tag{2}$$

where  $Z_t$  is a standardized time series,  $p, q, r, s$  are the positive integers indicating the BL order,  $\varphi, \theta, \beta$  are the model coefficients, and  $\varepsilon_t$  is a standardized stochastic series.

Considering  $\sum_{i=0}^r \sum_{j=1}^s (\beta_{ij} \cdot Z_{t-i-j} \cdot \varepsilon_{t-j})$  (i.e., the product of  $Z_t$  and  $\varepsilon_t$  in Eq. (2) causes the BL to be considered as a non-linear model (Ainkaran 2004); hence, it can be used in modeling non-linear phenomena such as streamflow.

Interested readers can refer to Fan and Yao (2003) for more details regarding the required steps of fitting a non-linear BL.

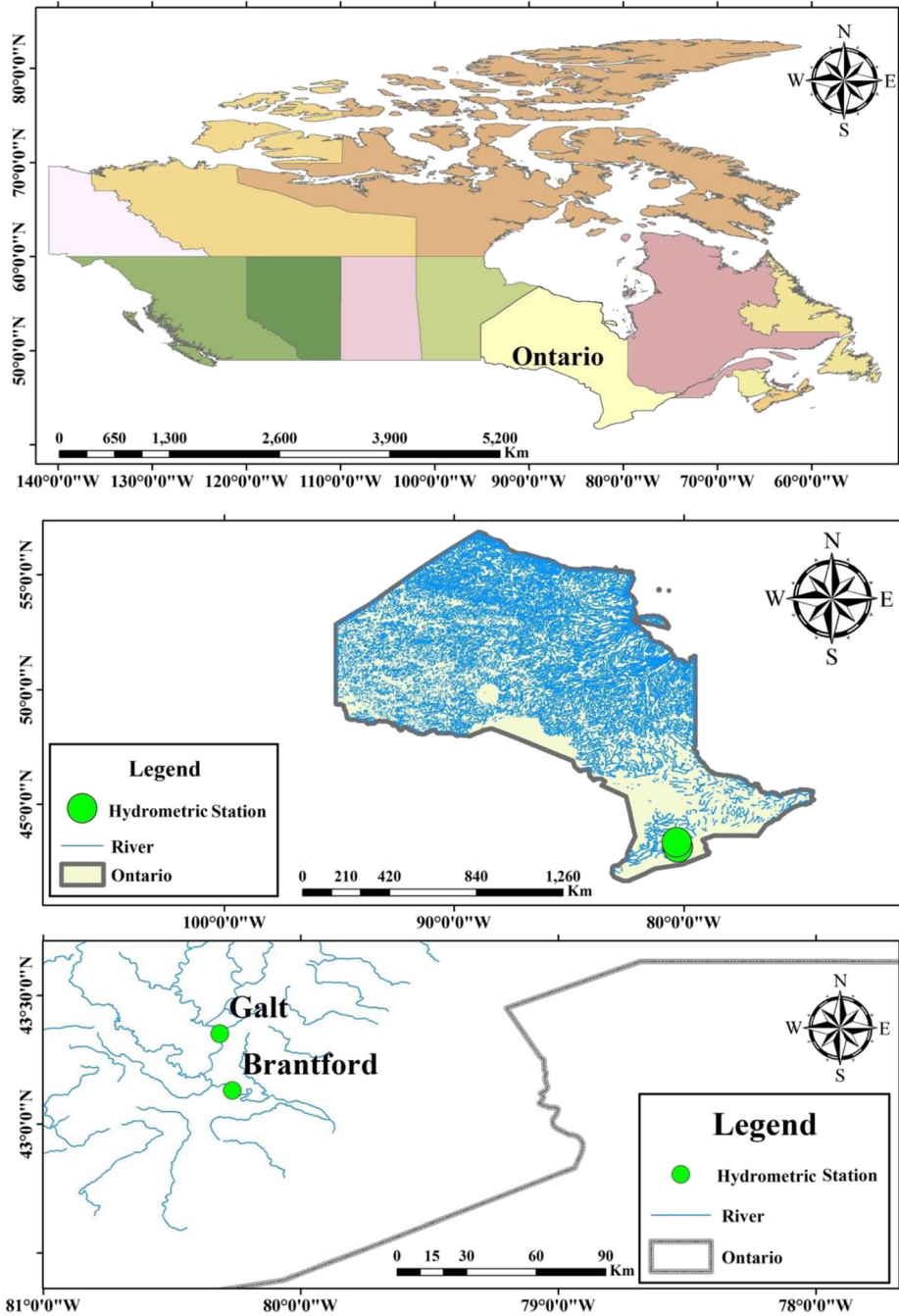


Fig. 1 Geographical locations of the hydrometric stations considered in this study

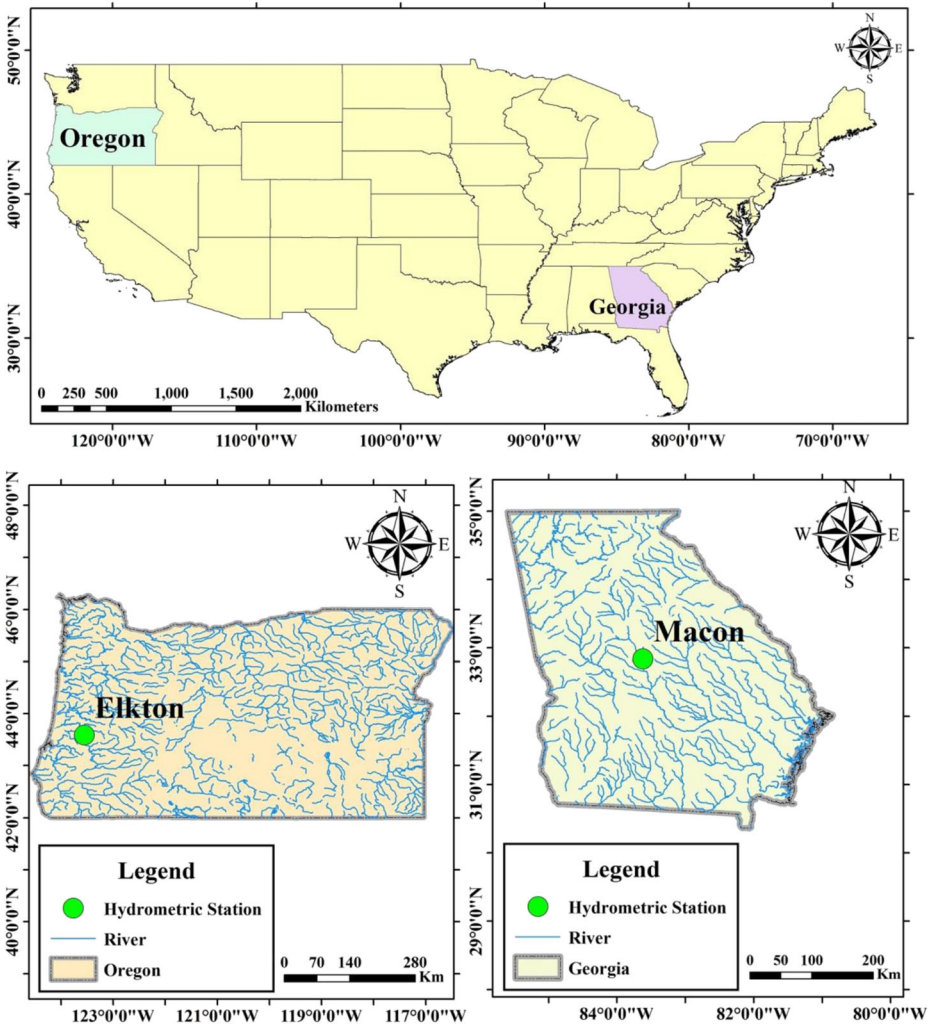


Fig. 1 (continued)

### 2.3 Multi-Layer Perceptron (MLP) Neural Network

MLP is known as one of the most common examples of feed-forward neural networks, the potential of which in modeling many engineering problems has been confirmed in recent years (Kisi et al. 2017; Jahani and Mohammadi 2019). In general, MLP consists of a sequential multi-layer network structure, including input layer, hidden/middle layer(s), and output layer. After obtaining information in the input layer, the information processing and model learning process begin in the hidden layer(s) with a number of neurons and activation functions. The type of activation function is selected with respect to the user experience, where sigmoid and linear functions are often used for the hidden and output layers, respectively.

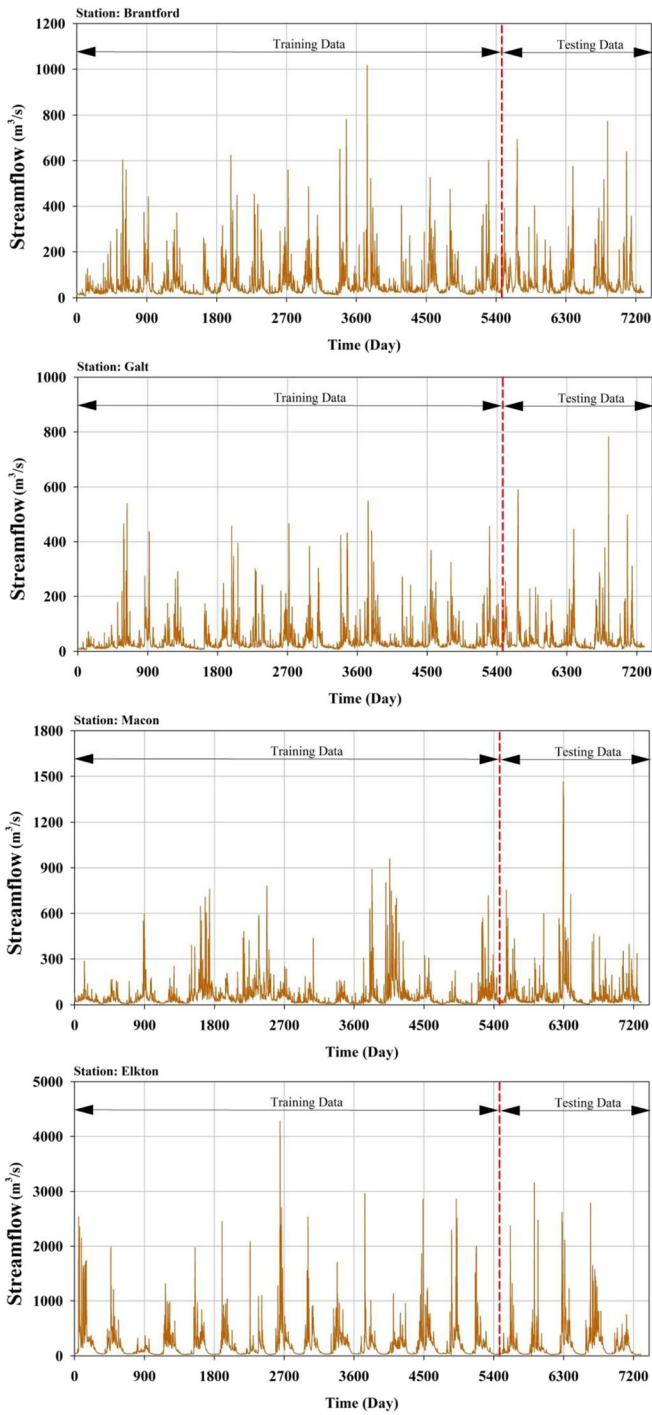


Fig. 2 Time series plots of the observed streamflows at the studied stations



Considering  $\varphi$  as an activation function of the  $j^{\text{th}}$  neuron in the hidden layer, the output of the neuron can be expressed as follows:

$$y_i = \varphi(\sum W_{ji}x_i + b_i) \quad (3)$$

where  $x_i$  is the input,  $W$  and  $b$  stand for the synaptic weight vector and bias, respectively. In this research, the Levenberg-Marquardt method is used to optimize the classic MLP structure (Kisi et al. 2016).

## 2.4 Particle Swarm Optimization (PSO)

The PSO meta-heuristic algorithm is firstly proposed by Eberhart and Kennedy (1995) for optimization of the complicated processes. It is a universal minimization method that can be used to deal with problems that are answered at one point or level in the next  $n$ -space. In such a space, hypotheses are made and an initial velocity is given to them. These particles then move in the response space, and the results are calculated based on a "merit criterion" after each time interval (Assareh et al. 2010). Over time, the particles accelerate toward particles that have a higher merit criterion and are in the same communication group. Although, each method works well in a range of issues, this method has shown great success in solving continuous optimization problems. Steps of the PSO algorithm in cloud: (i) Establishing and evaluating the primary population. (ii) Determine the best personal memories and the best collective memories. (iii) Speed and position update. (iv) If the conditions for stopping are not met, we will go to step 2.

## 2.5 Multi-Verse Optimizer (MVO)

This section introduces a brief overview of a newly developed nature-inspired algorithm named multi-verse optimizer (MVO), which was firstly proposed by Mirjalili et al. (2016). This algorithm is inspired focusing on three concepts in cosmology: the white hole, the black hole, and the wormhole. The mathematical relationships of these concepts are designed to perform local exploration, exploitation and search, respectively (Mirjalili et al. 2016). The fore mentioned concepts accomplish exploration, exploitation and local inspection based on the mathematical formulation so that there are two basic coefficients consisting of wormhole existence probability and travelling distance rate. The result of four challenging test problems on MVO algorithm show that the proposed algorithm is capable of delivering highly competitive results and is better than the best algorithms available in the literature in most tests (Faris et al. 2016). An interested reader can refer to Mirjalili et al. (2016) for more details about the MVO structure.

## 2.6 Models Development

As mentioned, the daily streamflow time series of the considered locations are modeled through the classical BL and MLP, as well as the boosted MLP-PSO, MLP-PSOMVO, and MLP-BL models. The below steps are followed for developing the classical and boosted models:

For the case of classical BL, various BL models containing the different orders are initially tested and fitted to the standardized daily streamflow data. Then, the optimal BL models are selected at each location focusing on the minimum values for the Akaike Information Criterion (AIC).

The classical MLP models at the study sites are developed by using the antecedent daily streamflows. In this regard, one-day to three-day lagged streamflow data (i.e.,  $Q_{t-1}$ ,  $Q_{t-2}$ ,  $Q_{t-3}$ ) is used for modeling the streamflow of present day (i.e.,  $Q_t$ ). The same input and output parameters are also employed when implementing the boosted models. Table 3 summarizes the input and output variables considered in the modeling procedure.

Regarding to use the PSO as an updator tool for weight of MLP, training phase of MLP should be improved and this is a reason for better training of classical MLP. In the boosted model of MLP-PSO, the PSO has an optimization role to find best optimal biases and weights for classical MLP model. In the boosted MLP-PSOMVO model, the search agents of weights and biases of the MLP model are calculated using the PSO and MOVO algorithms while the MLP uses benefits of PSO and MVO algorithms at same time. Then, PSOMVO can help to MLP for finding the optimal weights and biases and also the PSOMVO can find probable answers that the classical MLP and PSO have failed to provide it. So, these are reason for improving accuracy of MLP by new boosted PSOMVO method. Figure 3 shows a schematic diagram for input, output and modeling process via the classical MLP and boosted MLP-PSO and MLP-PSOMVO models implemented.

Finally, the modeled outputs of the classical MLP are summed with the residuals or stochastic errors of the classical BL to develop the boosted MLP-BL models as follows:

$$Q_{Hyb} = Q_{MLP} + Q_{BL} \tag{4}$$

where  $Q_{Hyb}$  presents the modeled daily streamflow via the boosted MLP-BL model,  $Q_{MLP}$  is the modeled daily streamflow by the classical MLP, and  $Q_{BL}$  illustrates the error of classical BL.

As already mentioned, the classical models are not able to capture the observed hydrological parameters time series such as streamflow with reliable precision. The classical time series (e.g., BL) and AI (e.g., MLP) models could have capability to modeling the stochastic and deterministic terms, respectively. The powerful modeling approaches are therefore needed to consider both the mentioned terms in the modeling procedure of hydrological parameters. The proposed MLP-BL models in this study apply both terms when modeling the daily streamflow.

As noted, whole the streamflow datasets are standardized before the modeling using Eq. (1). It is apparent that the modeled outputs of the daily streamflows via the classical and boosted models will be in the standardized forms. In other words, they must be de-standardized by multiplying the outputs of any modeling techniques by the corresponded standard deviations and then summing the resulting values by the corresponding averages.

**Table 3** Input and output parameters used to develop the classical and boosted models

Models	Models No.	Inputs	Output
MLP1, MLP1-PSO, MLP1-PSOMVO, MLP1-BL	M1	$Q_{t-1}$	$Q_t$
MLP2, MLP2-PSO, MLP2-PSOMVO, MLP2-BL	M2	$Q_{t-1}, Q_{t-2}$	$Q_t$
MLP3, MLP3-PSO, MLP3-PSOMVO, MLP3-BL	M3	$Q_{t-1}, Q_{t-2}, Q_{t-3}$	$Q_t$

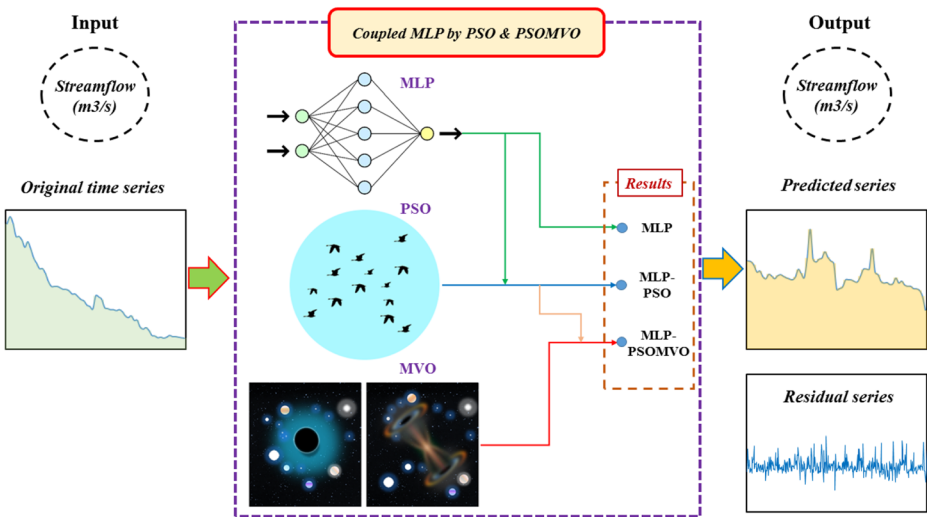


Fig. 3 The schematic diagram of modeling process by the classical MLP, and boosted MLP-PSO and MLP-PSOMVO techniques

### 2.7 Performance Evaluation Metrics

The root mean square error (RMSE), mean absolute error (MAE), and coefficient of determination ( $R^2$ ) are used in the present study to evaluate the accuracy of classical and proposed models in daily streamflow modeling as below:

$$RMSE = \sqrt{\frac{\sum_{i=1}^N (Q_{o,i} - Q_{m,i})^2}{N}} \tag{5}$$

$$MAE = \frac{\sum_{i=1}^N |Q_{o,i} - Q_{m,i}|}{N} \tag{6}$$

$$R^2 = \left[ \frac{\sum_{i=1}^N (Q_{o,i} - \overline{Q_o}) \cdot (Q_{m,i} - \overline{Q_m})}{\sqrt{\sum_{i=1}^N (Q_{o,i} - \overline{Q_o})^2 \cdot \sum_{i=1}^N (Q_{m,i} - \overline{Q_m})^2}} \right]^2 \tag{7}$$

where  $Q_{o, i}$ ,  $Q_{m, i}$ ,  $\overline{Q_o}$  and  $\overline{Q_m}$  indicate the  $i$ th observed daily streamflow, the  $i$ th modeled daily streamflow, the average of the observed daily streamflows, and the average of the modeled daily streamflows, respectively. Obviously, lower values achieved for the RMSE and MAE metrics, and the higher values obtained for the  $R^2$  illustrate the better performance of the applied modeling techniques in daily streamflow modeling.

### 3 Results

Firstly, the superior BL time series models are fitted to the observed streamflow data at the studied locations in their standardized forms. It is found that BL(13,4,1,1), BL(10,6,1,1), BL(10,0,1,1), and BL(12,1,1,1) are the best-performing BL models at the Brantford, Galt, Macon, and Elkton, respectively, with the minimum values for the AIC. The values of RMSE, MAE, and  $R^2$  metrics for both the train and test phases are calculated (Table 4). The highest and lowest accuracy levels of the developed BL models are respectively observed at the Galt and Elkton stations, respectively. The poorer performance of BL at the Elkton station (i.e., higher values of the RMSE and MAE, as well as the lower value of the  $R^2$ ) can be attributed to high streamflows of this location than the other stations.

Scatter plots for the observed against the modeled streamflow data via the BL model for each location during the test phase is depicted (Fig. 4). The dotted red lines in this Figure demonstrate the regression lines fitted to the observed and modeled streamflows. Furthermore, the equations provided in the form of  $y = ax + b$  are the equations of the regression lines in which  $y$  is the modeled streamflow,  $x$  is the observed streamflow,  $a$  is the slope, and  $b$  is the intercept. The better performance of each model is obtained when the values of  $a$  and  $b$  are closer to 1 and 0, respectively. This issue can be seen in the Brantford and Galt stations, while it cannot be concluded for the Macon and Elkton stations, specifically the Elkton, indicating the lower accuracy of the BL models developed at these locations.

The classical MLP is then used for modeling the daily streamflows of the studied locations with considering the input and output parameters mentioned in Table 3. In this context, different numbers for the hidden layer neurons are tested and then the optimal hidden layer neurons at each station are selected. It was found that the optimal numbers of neurons in the hidden layer for the classical MLP-based M1, M2, M3 models are 2, 30, 6 at Brantford, 14, 7, 20 at Galt, 18, 14, 20 at Macon, and 18, 3, 7 at Elkton, respectively. The values of RMSE, MAE, and  $R^2$  statistics computed for the conventional MLP during both train and test phases are listed in the first sections of Tables 5, 6, 7 and 8. The results denote the applicability of antecedent daily streamflow values for the streamflow modeling of each day at any location. Moreover, assessing the accuracy of MLP models developed under models No. M1-M3 indicates that the modeling accuracy of daily streamflow improves with increasing the number of lags.

As previously mentioned, the main aim of the current study is to increase the performance of classical MLP for modeling the daily streamflow. To that end, the boosted MLP-PSO, MLP-PSOMVO, and MLP-BL models are developed. The values of statistical metrics obtained for the aforementioned boosted models are tabulated in the second to fourth sections of the Tables 5, 6, 7 and 8. As clearly can be seen, the higher values of the RMSE and MAE, as

**Table 4** Values of RMSE, MAE, and  $R^2$  statistics obtained for the BL models at the studied sites during train and test phases

Stations	Models	Train			Test		
		RMSE (m <sup>3</sup> /s)	MAE (m <sup>3</sup> /s)	$R^2$	RMSE (m <sup>3</sup> /s)	MAE (m <sup>3</sup> /s)	$R^2$
Brantford	BL(13,4,1,1)	33.192	17.835	0.805	32.983	17.829	0.835
Galt	BL(10,6,1,1)	25.608	12.949	0.771	24.556	12.747	0.841
Macon	BL(10,0,1,1)	35.370	20.054	0.849	44.981	22.442	0.870
Elkton	BL(12,1,1,1)	144.436	66.793	0.724	162.507	74.214	0.692

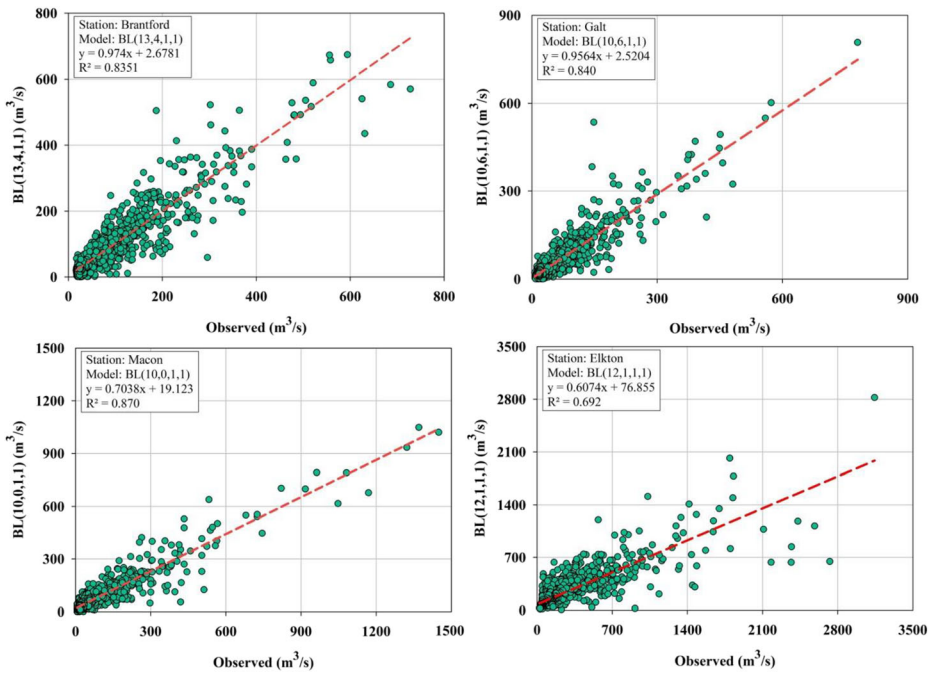


**Fig. 4** Scatter plots for the observed versus modeled streamflow data by the BL models at the studied stations during the test phase

well as the lower values of  $R^2$  are significantly improved through the proposed models than those of the corresponding metrics in the classical MLP.

Here, the performance of all the classical and boosted models implemented in this study is evaluated for the daily streamflow modeling of the considered locations. The BL time series models developed at all stations perform weaker than the classical MLP. A comparative assessment of the classical MLP and boosted MLP-based models illustrates that the boosted models including the MLP-PSO, MLP-PSOMVO, and MLP-BL outperform the classical MLP in daily streamflow modeling. In this context, the MLP-PSOMVO models present

**Table 5** Values of RMSE, MAE, and  $R^2$  statistics obtained at the Brantford station during train and test phases

Models	Models No.	Train			Test		
		RMSE (m <sup>3</sup> /s)	MAE (m <sup>3</sup> /s)	$R^2$	RMSE (m <sup>3</sup> /s)	MAE (m <sup>3</sup> /s)	$R^2$
MLP	M1	27.556	12.859	0.845	27.294	13.246	0.872
	M2	23.604	11.360	0.886	24.382	11.987	0.897
	M3	22.823	10.957	0.894	<b>23.254</b>	<b>11.476</b>	<b>0.907</b>
MLP-PSO	M1	25.337	12.200	0.869	23.744	12.025	0.903
	M2	19.187	9.329	0.925	<b>16.728</b>	<b>8.926</b>	<b>0.952</b>
	M3	19.579	9.493	0.922	17.523	9.265	0.947
MLP-PSOMVO	M1	18.148	8.858	0.933	<b>15.802</b>	<b>8.285</b>	<b>0.957</b>
	M2	18.092	8.956	0.933	16.253	8.865	0.954
	M3	18.155	9.142	0.933	16.717	9.168	0.952
MLP-BL	M1	11.768	5.775	0.972	12.223	5.930	0.974
	M2	7.987	4.189	0.988	8.402	4.529	0.989
	M3	5.998	3.251	0.993	<b>6.426</b>	<b>3.530</b>	<b>0.994</b>

**Table 6** Values of RMSE, MAE, and R<sup>2</sup> statistics obtained at the Galt station during train and test phases

Models	Models No.	Train			Test		
		RMSE (m <sup>3</sup> /s)	MAE (m <sup>3</sup> /s)	R <sup>2</sup>	RMSE (m <sup>3</sup> /s)	MAE (m <sup>3</sup> /s)	R <sup>2</sup>
MLP	M1	21.388	9.588	0.821	21.376	9.735	0.868
	M2	19.053	8.693	0.858	19.388	9.039	0.892
	M3	18.527	8.598	0.866	<b>19.069</b>	<b>8.979</b>	<b>0.894</b>
MLP-PSO	M1	19.285	9.114	0.855	18.196	9.021	0.905
	M2	14.762	7.085	0.915	<b>12.941</b>	<b>6.698</b>	<b>0.952</b>
	M3	15.408	7.389	0.908	13.442	7.047	0.948
MLP-PSOMVO	M1	13.406	6.567	0.930	11.752	6.109	0.960
	M2	13.691	6.674	0.927	12.111	6.407	0.957
	M3	12.812	6.287	0.936	<b>11.358</b>	<b>6.139</b>	<b>0.962</b>
MLP-BL	M1	7.879	3.771	0.976	8.344	3.957	0.980
	M2	5.237	2.857	0.990	<b>6.067</b>	<b>3.190</b>	<b>0.990</b>
	M3	5.490	2.771	0.989	6.386	3.117	0.990

superior performances in comparison to the MLP-PSO ones at all the study locations; however, the boosted MLP-BL models are the best-performing boosted paradigms with the highest degree of precision. The only exception is observed at the Macon station, where the boosted MLP-PSOMVO models present the best results. The superior models for high-performance streamflow modeling are related to the models no. of M3 (MLP-BL) at the Brantford, M2 (MLP-BL) at the Galt, M3 (MLP-PSOMVO) at the Macon, and M2 (MLP-BL) at the Elkton. As an example, the RMSE values of aforementioned superior boosted models in comparison to the corresponding models of classical MLP are reduced in the train and test phases by 73.719% and 72.366% for the Brantford, 72.513% and 68.707% for the Galt, 31.147% and 37.719% for the Macon, 73.823% and 72.719% for the Elkton.

In order to graphically assess the efficiencies of classical MLP and boosted MLP-based models, the scatter and radar diagrams are prepared (Figs. 5, 6 and 7). In doing so, the best-performing classical MLP and boosted MLP-PSO, MLP-PSOMVO, and MLP-BL models at each station during the test phase is selected to prepare the scatter plots. The error criteria of the superior models are highlighted in boldface in Tables 5, 6, 7 and 8. Clearly, lesser dispersions of the data, higher values of the slopes, and lower values for the intercepts in the fitted regression lines of the boosted models than those of the classical MLP ones denote the

**Table 7** Values of RMSE, MAE, and R<sup>2</sup> statistics obtained at the Macon station during train and test phases

Models	Models No.	Train			Test		
		RMSE (m <sup>3</sup> /s)	MAE (m <sup>3</sup> /s)	R <sup>2</sup>	RMSE (m <sup>3</sup> /s)	MAE (m <sup>3</sup> /s)	R <sup>2</sup>
MLP	M1	31.226	14.981	0.864	40.380	18.764	0.870
	M2	27.852	13.720	0.891	36.907	16.948	0.891
	M3	27.071	13.426	0.897	<b>34.991</b>	<b>16.300</b>	<b>0.902</b>
MLP-PSO	M1	26.961	13.734	0.899	33.529	16.173	0.910
	M2	22.740	11.421	0.928	28.564	13.600	0.935
	M3	21.290	11.141	0.937	<b>27.276</b>	<b>13.268</b>	<b>0.941</b>
MLP-PSOMVO	M1	20.475	10.536	0.941	25.903	12.203	0.946
	M2	19.177	10.198	0.949	<b>22.986</b>	<b>11.425</b>	<b>0.958</b>
	M3	17.975	9.912	0.955	24.954	12.065	0.951
MLP-BL	M1	21.058	11.671	0.968	27.167	12.901	0.973
	M2	19.674	10.939	0.983	25.552	12.397	0.988
	M3	19.186	10.833	0.986	<b>24.441</b>	<b>11.825</b>	<b>0.990</b>

**Table 8** Values of RMSE, MAE, and  $R^2$  statistics obtained at the Elkton station during train and test phases

Models	Models No.	Train			Test		
		RMSE (m <sup>3</sup> /s)	MAE (m <sup>3</sup> /s)	$R^2$	RMSE (m <sup>3</sup> /s)	MAE (m <sup>3</sup> /s)	$R^2$
MLP	M1	124.468	42.702	0.791	132.775	45.907	0.789
	M2	120.661	41.149	0.804	<b>126.589</b>	<b>43.563</b>	<b>0.808</b>
	M3	113.361	40.313	0.826	127.664	43.441	0.804
MLP-PSO	M1	79.062	27.974	0.915	<b>97.713</b>	<b>29.921</b>	<b>0.885</b>
	M2	84.867	31.089	0.902	101.381	32.856	0.878
	M3	89.308	32.244	0.892	100.499	33.640	0.882
MLP-PSOMVO	M1	66.075	24.226	0.941	90.310	26.205	0.902
	M2	67.859	23.968	0.938	83.396	24.488	0.917
	M3	76.068	26.629	0.922	<b>81.258</b>	<b>27.313</b>	<b>0.921</b>
MLP-BL	M1	42.910	16.019	0.975	46.293	17.984	0.974
	M2	31.585	13.938	0.987	<b>34.535</b>	<b>14.878</b>	<b>0.986</b>
	M3	34.692	13.495	0.984	38.118	15.064	0.983

dependable performances of the boosted models for the daily streamflow modeling. In addition, radar diagrams are provided to illustrate how the values of RMSE metric change in the classical MLP and implemented proposed models (Fig. 7). For this goal, the RMSE values of all the models under models no. M1-M3 during the test phase are used. The radar diagrams in this study are as a triangular since three types of models (i.e., M1, M, M3) are considered when modeling the daily streamflow. As obviously can be seen, triangles made for the classical MLP models at the studied locations are large indicating the highest values of RMSE and therefore lowest accuracy of the classical MLP. However, these triangles are much denser in the boosted models, especially for the boosted MLP-BL and MLP-PSOMVO models. This point confirms the suitability of boosted models compared to the classical MLP for modeling the daily streamflow time series with a reliable precision.

## 4 Discussion

As concluded, the performance of classic MLP at the studied stations was found to be better than the classic BL. This result could be due to the time scale of the data used (i.e., daily), so that contradictory results may be achieved considering other time scales including the monthly, seasonally, etc. Superior performances of the linear and non-linear types of time series models compared to the AI techniques were reported by some researchers on a monthly time scale. In this regard, the linear AR model illustrated higher accuracy than the AI-based models (GEP, FFNN, RBFN, ANFIS) applied to monthly streamflow modeling (Terzi and Ergin 2014). Moreover, the capability of linear FARIMA as well as non-linear SETAR and GARCH time series-based models for monthly streamflow modeling was better than the MARS, GEP, ANN, and RF (Mehdizadeh et al. 2019b; Fathian et al. 2019).

As is apparent, the modeled streamflow data using any modeling techniques such as MLP could show deviations from the observed data. Hence, the main purpose of this study was to improve the daily streamflow modeling via coupling the MLP with three techniques including the time series-based BL, as well as two optimization-based PSO and PSOMVO. Superior performances of the boosted MLP-PSO and MLP-PSOMVO models than the classical MLP can be explained taking into account the fact that PSOMVO with global and local search capability at the same time can train MLP by minimum error. As a result, the proposed method

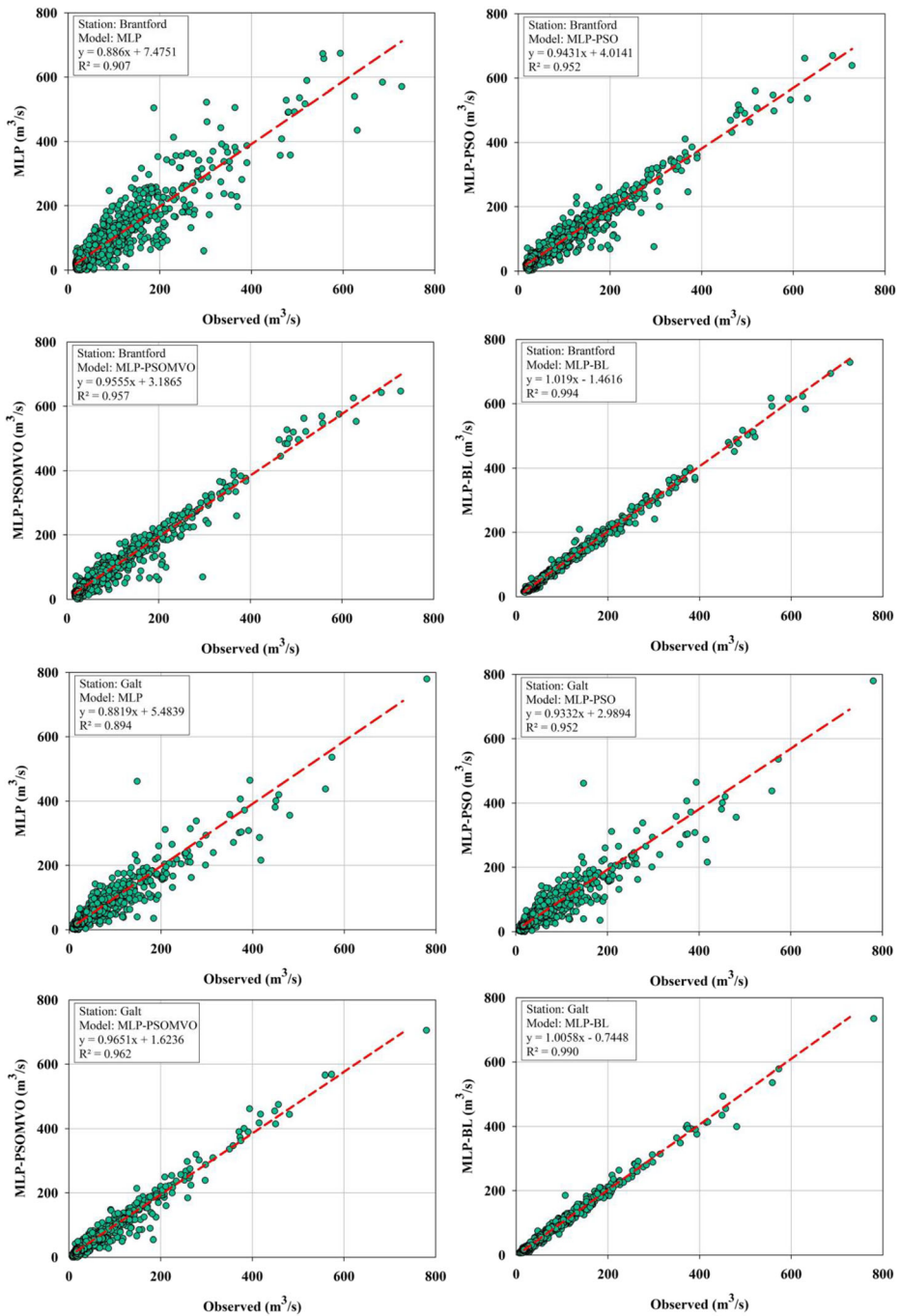


**Fig. 5** Scatter plots for the observed versus modeled streamflow data by the best-performing classical MLP and boosted MLP-based models at the Canadian stations (Brantford and Galt) during the test phase



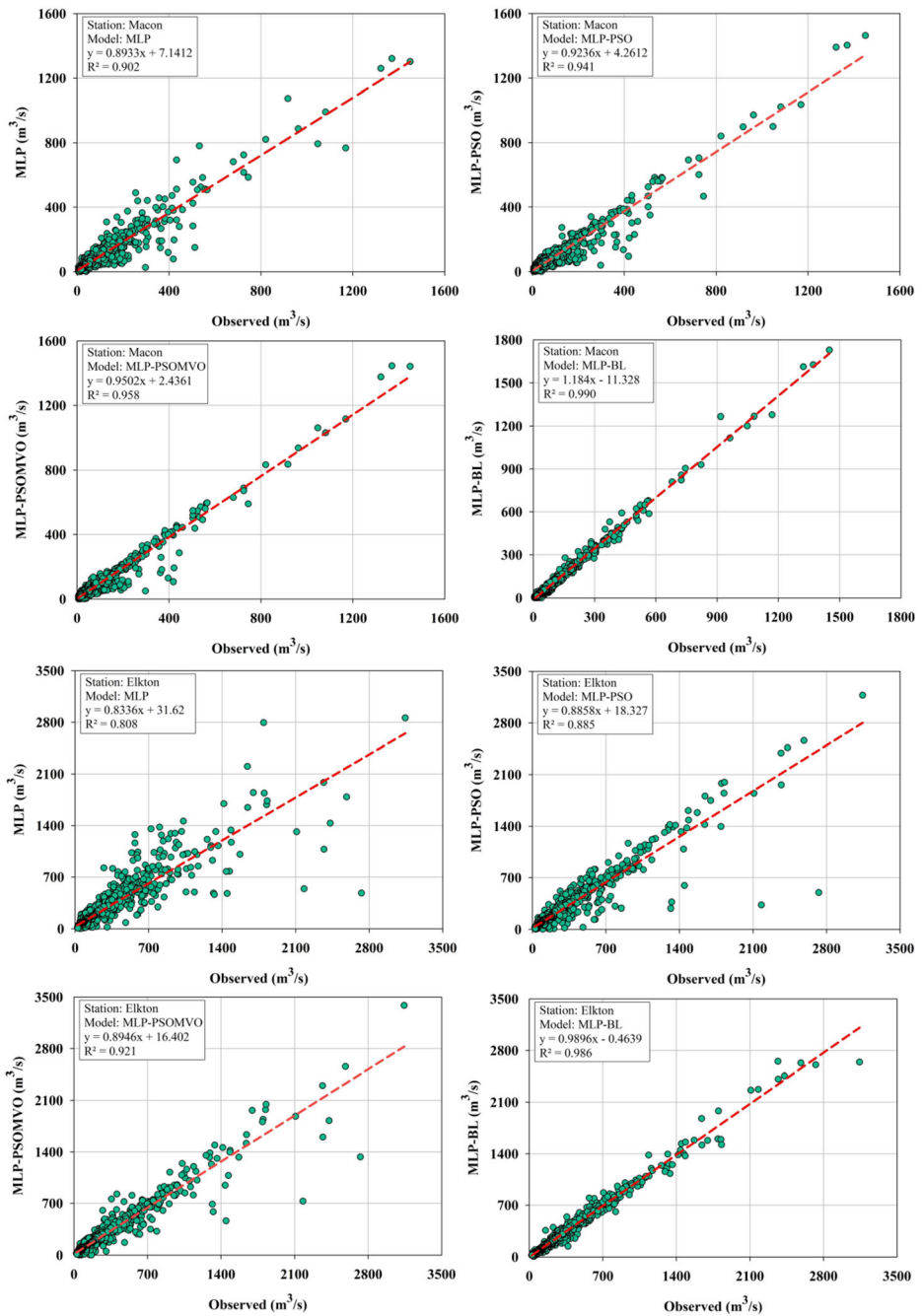


**Fig. 6** Scatter plots for the observed versus modeled streamflow data by the best-performing classical MLP and boosted MLP-based models at the USA stations (Macon and Elkton) during the test phase

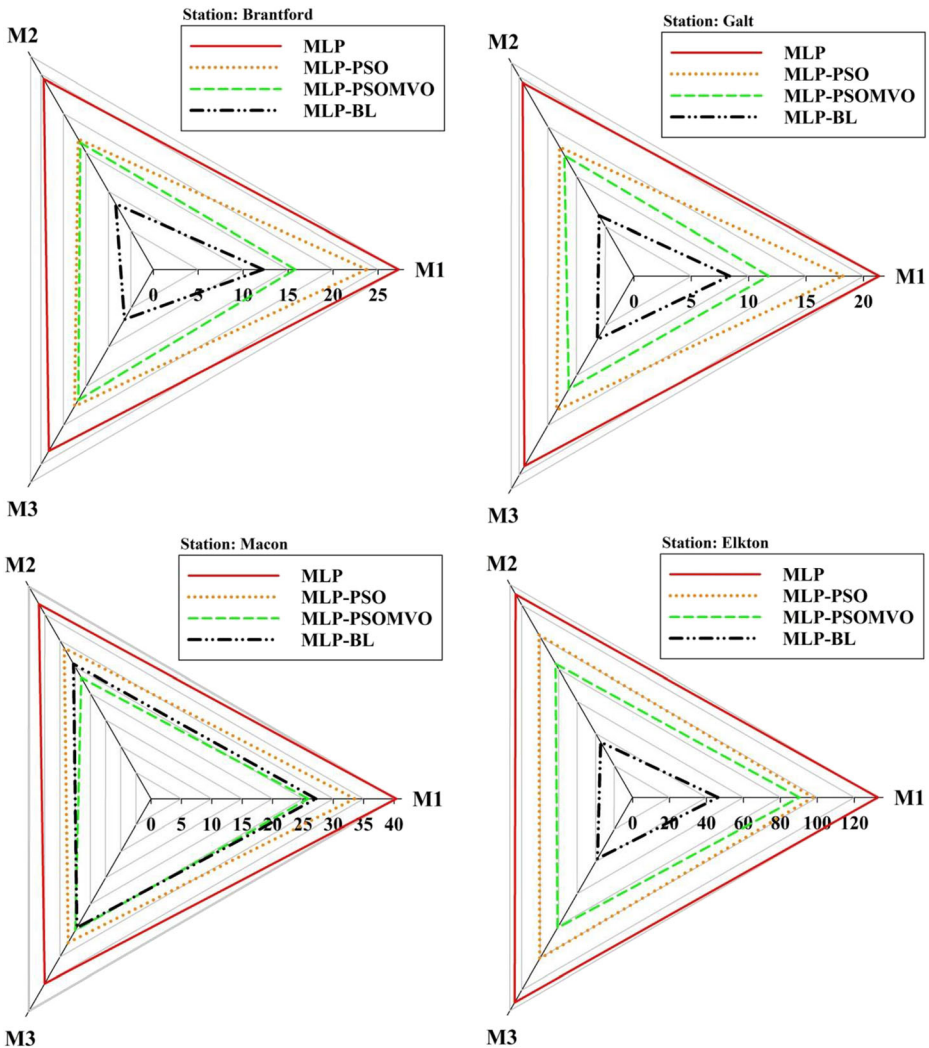


Fig. 7 Radar diagrams for the RMSE values of the classical MLP and boosted MLP-based models at the studied stations during the test phase

can find the optimal values of the desired function and is a suitable learning algorithm for the classical MLP. The classical MLP has better learning with PSOMVO which leads to higher accuracy of streamflow modeling. On the other hand, considering both the stochastic and deterministic terms via the boosted MLP-BL can be the most important reason for the higher modeling accuracy of the boosted models compared to the classical MLP when modeling the daily streamflow.

One of the results of boosted models (i.e., reliable accuracy of the boosted MLP-BL than the classical MLP) supports the outcomes concluded in previous works. For example, MARS and GEP models were coupled on the ARCH time series model for reference evapotranspiration estimation (Mehdzizadeh 2018). The linear AR, MA, and ARMA time series models were hybridized with the MARS and K-nearest neighbors (KNN) approaches to precipitation

modeling (Mehdizadeh 2020). The performance of GEP and Bayesian network (BN) models was improved for streamflow modeling through coupling the mentioned AI models with the linear AR and ARMA (Mehdizadeh and Kozekalani Sales 2018). In other studies, hybrid models were proposed by combining the various time series models including the linear FARIMA as well as non-linear ARCH, GARCH, and SETAR with the diverse types of AI models such as MARS, GEP, and ANN to precipitation and streamflow modeling (Mehdizadeh et al. 2017, 2018, 2019b). Improvements in the performance of AI techniques via the boosted AI-time series models were reported by the scholars.

Furthermore, higher performance of the boosted models developed through coupling the AI and optimization-based models compared to the standalone AI models was confirmed and reported by some scholars. For example, a new boosted model based on coupling shuffled frog leaping algorithm (SFLA) and ANFIS was implemented for predicting streamflow in two rivers in Vietnam (Mohammadi et al. 2020). A boosted technique was proposed by integrating the MARS and DE as an optimization approach (i.e., MARS-DE) for monthly streamflow estimation of Tigris River, Iraq (Al-Sudani et al. 2019). The proposed boosted model achieved better estimates of the streamflow than the standalone MARS. In another study, boosted models were developed via coupling the GWO method with the AI-based SVM, ANN, and MLR for estimating the monthly streamflow of Aswan High Dam, Egypt (Tikhamarine et al. 2019a). The results denoted the superior performance of the proposed models than the standalone ones. Also, there are other nature-inspired algorithms as they recently developed by researchers in hydrological studies. For example, the SVR model was developed by Krill Herd algorithm (SVR-KHA) for daily solar radiation estimation in Iran (Mohammadi and Aghashariatmadari 2020). The ANFIS model was modified by Grey Wolf Optimizer algorithm (ANFIS-GWO) for soil moisture simulating (Maroufpoor et al. 2020). The MLP model was extended by Whale Optimization Algorithm (MLP-WOA) for predicting of field capacity and the permanent wilting point (Vaheddoost et al. 2020).

One of the main flaws of the classical AI models such as MLP applied in the current study is their weaknesses in modeling the extreme values of the hydrological time series such as streamflow. The extreme values of the streamflow time series include the droughts and floods. Knowing the extreme streamflows (i.e., high and low values) in each river is very important and could be of use to design water resources structures like dam spillway and sluiceway operations (Kisi and Sanikhani 2012). Evaluating the performance of classical MLP models in modeling the extreme values demonstrate that the classical MLP models developed at whole the study stations provide the over-estimation and under-estimation in modeling the low and peak streamflow data. However, the boosted models developed show superior performances in capturing the observed daily streamflow time series, specifically for the high values (i.e., floods). In this regard, one of the most important reasons for the low performance of the classical MLP models is their poorer ability to model the high values, while the boosted models illustrate an acceptable capability for modeling the peak values of the streamflow time series. This is clearly observed in the scatter plots illustrated in Figs. 5 and 6.

## 5 Conclusions

In the present study, the daily streamflow time series of four hydrometric stations consisting of the Brantford and Galt in Canada, as well as Macon and Elkton in United States were modeled. Two classical models and three boosted paradigms are used as modeling techniques. Assessing

the accuracy of classical models, namely the time series-based BL and an AI-based MLP illustrated that the MLP performed better than the BL for the daily streamflow modeling of the studied sites. The boosted models were then developed and proposed for improving the streamflow models (i.e., MLP-PSO, MLP-PSOMVO, and MLP-BL) were found to provide better results compared to the classical MLP. In general, the boosted MLP-BL outperformed both the other boosted models at the studied locations, except for the Macon station where the MLP-PSOMVO was the best-performing boosted model.

As clearly concluded, the proposed models showed reliable performances than the classical models used in this study. More boosted models are suggested to be implemented in future research works to improve the modeling accuracy of hydrological variables time series such as streamflow. In this context, coupling the AI-based models with the wavelet analysis, other types of the time series models and optimization algorithms could be of use. The modeling accuracy of proposed models could also be examined on the other time scales such as the monthly and seasonally. in modeling the streamflow. Additionally, it is suggested to test the performance of proposed models for modeling the other hydrological variables including rainfall, evaporation, evapotranspiration, etc.

## Compliance with Ethical Standards

**Conflict of Interest** The authors declare no conflicts of interest.

## References

- Abdollahi S, Raeisi J, Khalilianpour M, Ahmadi F, Kisi O (2017) Daily mean Streamflow prediction in perennial and non-perennial Rivers using four data driven techniques. *Water Resour Manage* 31(15):4855–4874
- Abudu S, Cui C-l, King JP, Abudukadeer K (2010) Comparison of performance of statistical models in forecasting monthly streamflow of Kizil River, China. *Water Sci Eng* 3(3):269–281
- Adamowski A, Chan HF, Prasher SO, Sharda VN (2012) Comparison of multivariate adaptive regression splines with coupled wavelet transform artificial neural networks for runoff forecasting in Himalayan micro-watersheds with limited data. *J Hydroinf* 14(3):731–744
- Aghelpour P, Mohammadi B, Biazar SM (2019) Long-term monthly average temperature forecasting in some climate types of Iran, using the models SARIMA, SVR, and SVR-FA. *Theor Appl Climatol* 138(3–4):1471–1480
- Aghelpour P, Bahrami-Pichaghchi H, Kisi O (2020) Comparison of three different bio-inspired algorithms to improve ability of neuro fuzzy approach in prediction of agricultural drought, based on three different indexes. *Comput Electron Agric* 170:105279
- Ainkaran P (2004) Analysis of some linear and nonlinear time series models. A thesis submitted in fulfillment of the requirements for the degree of Master of Science, School of Mathematics and Statistics, University of Sydney
- Al-Sudani ZA, Salih SQ, Sharafati A, Yaseen ZM (2019) Development of multivariate adaptive regression spline integrated with differential evolution model for streamflow simulation. *J Hydrol* 573:1–12
- Anghileri D, Voisin N, Castelletti A, Pianosi F, Nijssen B, Lettenmaier DP (2016) Value of long-term streamflow forecasts to reservoir operations for water supply in snow-dominated river catchments. *Water Resour Res* 52(6):4209–4225
- Assareh E, Behrang MA, Assari MR, Ghanbarzadeh A (2010) Application of PSO (particle swarm optimization) and GA (genetic algorithm) techniques on demand estimation of oil in Iran. *Energy* 35(12):5223–5229
- Bayazit M (2015) Nonstationarity of hydrological records and recent trends in trend analysis: a state-of-the-art review. *Environ Process* 2(3):527–542
- Choong SM, El-Shafie A, Mohtar WW (2017) Optimisation of multiple hydropower reservoir operation using artificial bee colony algorithm. *Water Resour Manag* 31(4):1397–1411

- Di C, Yang X, Wang X (2014) A four-stage hybrid model for hydrological time series forecasting. *PLoS One* 9(8):e104663
- Eberhart R, Kennedy J (1995) Particle swarm optimization. In *Proceedings of the IEEE international conference on neural networks* 4:1942–1948
- Fan J, Yao Q (2003) *Nonlinear time series, nonparametric and parametric methods*. Springer-Verlag, New York, Inc.
- Fang W, Huang S, Ren K, Huang Q, Huang G, Cheng G, Li K (2019) Examining the applicability of different sampling techniques in the development of decomposition-based streamflow forecasting models. *J Hydrol* 568:534–550
- Faris H, Aljarah I, Mirjalili S (2016) Training feedforward neural networks using multi-verse optimizer for binary classification problems. *Appl Intell* 45:322–332
- Fathian F, Mehdizadeh S, Kozekalani Sales A, Safari MJS (2019) Hybrid models to improve the monthly river flow prediction: integrating artificial intelligence and non-linear time series model. *J Hydrol* 575:1200–1213
- Garcia M, Portney K, Islam S (2016) A question driven socio-hydrological modeling process. *Hydrol Earth Syst Sci* 20(1):73–92
- Granger CWJ, Andersen A (1978) Non-linear time series modelling. In *applied time series analysis I* (pp. 25–38). Academic press
- Hadi SJ, Tombul M (2018) Monthly streamflow forecasting using continuous wavelet and multi-gene genetic programming combination. *J Hydrol* 561:674–687
- He Z, Wen X, Liu H, Du J (2014) A comparative study of artificial neural network, adaptive neuro fuzzy inference system and support vector machine for forecasting river flow in the semiarid mountain region. *J Hydrol* 509:379–386
- Jahani B, Mohammadi B (2019) A comparison between the application of empirical and ANN methods for estimation of daily global solar radiation in Iran. *Theor Appl Climatol* 137(1–2):1257–1269
- Kisi O, Sanikhani H (2012) River flow estimation and forecasting by using two different adaptive neuro-fuzzy approaches. *Water Resour Manag* 26:1715–1729
- Kisi O, Nia AM, Goshen MG, Tajabadi MRJ, Ahmadi A (2012) Intermittent streamflow forecasting by using several data driven techniques. *Water Resour Manag* 26(2):457–474
- Kisi O, Genc O, Dinc S, Zounemat-Kermani M (2016) Daily pan evaporation modeling using chi-squared automatic interaction detector, neural networks, classification and regression tree. *Comput Electron Agric* 122:112–117
- Kisi O, Sanikhani H, Cobaner M (2017) Soil temperature modeling at different depths using neuro-fuzzy, neural network, and genetic programming techniques. *Theor Appl Climatol* 129(3–4):833–848
- Liu Z, Zhou P, Chen G, Guo L (2014) Evaluating a coupled discrete wavelet transform and support vector regression for daily and monthly streamflow forecasting. *J Hydrol* 519(D):2822–2831
- Maroufpoor S, Bozorg-Haddad O, Maroufpoor E (2020) Reference evapotranspiration estimating based on optimal input combination and hybrid artificial intelligent model: hybridization of artificial neural network with grey wolf optimizer algorithm *Journal of Hydrology*, 125060. 10.1016/j.jhydrol.2020.125060, 588
- Mehdizadeh S (2018) Estimation of daily reference evapotranspiration ( $ET_0$ ) using artificial intelligence methods: offering a new approach for lagged  $ET_0$  data-based modeling. *J Hydrol* 559:794–812
- Mehdizadeh S (2020) Using AR, MA, and ARMA time series models to improve the performance of MARS and KNN approaches in monthly precipitation modeling under limited climatic data. *Water Resour Manag* 34: 263–282 <https://doi.org/10.1007/s11269-019-02442-1>
- Mehdizadeh S, Kozekalani Sales A (2018) A comparative study of autoregressive, autoregressive moving average, gene expression programming and Bayesian networks for estimating monthly streamflow. *Water Resour Manag* 32(9):3001–3022
- Mehdizadeh S, Behmanesh J, Khalili K (2017) A comparison of monthly precipitation point estimates using integration of soft computing methods and GARCH time series model. *J Hydrol* 554:721–742
- Mehdizadeh S, Behmanesh J, Khalili K (2018) New approaches for estimation of monthly rainfall based on GEP-ARCH and ANN-ARCH hybrid models. *Water Resour Manag* 32(2):527–545
- Mehdizadeh S, Fathian F, Safari MJS, Adamowski JF (2019a) Comparative assessment of time series and artificial intelligence models to estimate monthly streamflow: a local and external data analysis approach. *J Hydrol* 579:124225
- Mehdizadeh S, Fathian F, Adamowski JF (2019b) Hybrid artificial intelligence-time series models for monthly streamflow modeling. *Appl Soft Comput* 80:873–887
- Mirjalili S, Mirjalili SM, Hatamlou A (2016) Multi-verse optimizer: a nature-inspired algorithm for global optimization. *Neural Comput Appl* 27(2):495–513
- Moazenzadeh R, Mohammadi B (2019) Assessment of bio-inspired metaheuristic optimisation algorithms for estimating soil temperature. *Geoderma* 353:152–171

- Moazenazadeh R, Mohammadi B, Shamshirband S, Chau KW (2018) Coupling a firefly algorithm with support vector regression to predict evaporation in northern Iran. *Eng Appl Comput Fluid Mech* 12(1):584–597
- Mohammadi B (2019a) Predicting total phosphorus levels as indicators for shallow lake management. *Ecol Indic* 107:105664
- Mohammadi B (2019b) “Prediction of effective climate change indicators using statistical downscaling approach and impact assessment on pearl millet (*Pennisetum glaucum* L.) yield through genetic algorithm in Punjab, Pakistan” by Asmat Ullah, Nasrin Salehnia, Sohrab Kolsoumi, Ashfaq Ahmad, Tasneem Khaliq. *Ecol Indic* 101:973–974
- Mohammadi B, Aghashariatmadari Z (2020) Estimation of solar radiation using neighboring stations through hybrid support vector regression boosted by krill herd algorithm. *Arab J Geosci* 13:363. <https://doi.org/10.1007/s12517-020-05355-1>
- Mohammadi B, Mehdizadeh S (2020) Modeling daily reference evapotranspiration via a novel approach based on support vector regression coupled with whale optimization algorithm. *Agric Water Manag* 237:106145. <https://doi.org/10.1016/j.agwat.2020.106145>
- Mohammadi B, Linh NTT, Pham QB, Ahmed AN, Vojteková J, Guan Y, Abba SI, El-Shafie A (2020) Adaptive neuro-fuzzy inference system coupled with shuffled frog leaping algorithm for predicting river streamflow time series. *Hydrol Sci J*:1–14. <https://doi.org/10.1080/02626667.2020.1758703>
- Peugeot C, Cappelaere B, Vieux BE, Séguis L, Maia A (2003) Hydrologic process simulation of a semiarid, endoreic catchment in Sahelian West Niger. 1. Model-aided data analysis and screening. *J Hydrol* 279(1–4): 224–243
- Pham QB, Afan HA, Mohammadi B, Ahmed AN, Linh NTT, Vo ND, ... El-Shafie A (2020) Hybrid model to improve the river streamflow forecasting utilizing multilayer perceptron-based intelligent water drop optimization algorithm. <https://doi.org/10.1007/s00500-020-05058-5>
- Siqueira H, Boccato L, Luna I, Attux R, Lyra C (2018) Performance analysis of unorganized machines in streamflow forecasting of Brazilian plants. *Appl Soft Comput* 68:494–506
- Terzi O, Ergin G (2014) Forecasting of monthly river flow with autoregressive modeling and data-driven techniques. *Neural Comput Applic* 25:179–188
- Tikhmarine Y, Souag-Gamane D, Ahmed AN, Kisi O, El-Shafie A (2019a) Improving artificial intelligence models accuracy for monthly streamflow forecasting using grey wolf optimization (GWO) algorithm. *J Hydrol* 582:124435
- Tikhmarine Y, Malik A, Kumar A, Souag-Gamane D, Kisi O (2019b) Estimation of monthly reference evapotranspiration using novel hybrid machine learning approaches. *Hydrol Sci J* 64(15):1824–1842
- Tongal H, Booi MJ (2018) Simulation and forecasting of streamflows using machine learning models coupled with base flow separation. *J Hydrol* 564:266–282
- Uysal G, Forman AA, Fensoy A (2016) Streamflow forecasting using different neural network models with satellite data for a snow dominated region in Turkey. *Procedia Eng* 154:1185–1192
- Vaheddoost B, Guan Y, Mohammadi B (2020) Application of hybrid ANN-whale optimization model in evaluation of the field capacity and the permanent wilting point of the soils. *Sci Pollut Res* 27:13131–13141. <https://doi.org/10.1007/s11356-020-07868-4>
- Wang S, Huang G, Baetz B, Huang W (2016) Probabilistic inference coupled with possibilistic reasoning for robust estimation of hydrologic parameters and piecewise characterization of interactive uncertainties. *J Hydrometeorol* 17(4):1243–1260
- Yaseen ZM, Kisi O, Demir V (2016) Enhancing long-term streamflow forecasting and predicting using periodicity data component: application of artificial intelligence. *Water Resour Manag* 30(12):4125–4151
- Zhang H, Singh VP, Wang B, Yu Y (2016) CEREF: a hybrid data-driven model for forecasting annual streamflow from a socio-hydrological system. *J Hydrol* 540:246–256

## Affiliations

**Babak Mohammadi<sup>1</sup> · Farshad Ahmadi<sup>2</sup> · Saeid Mehdizadeh<sup>3</sup> · Yiqing Guan<sup>1</sup> · Quoc Bao Pham<sup>4,5</sup> · Nguyen Thi Thuy Linh<sup>6</sup> · Doan Quang Tri<sup>7</sup>**

<sup>1</sup> College of Hydrology and Water Resources, Hohai University, Nanjing 210098, China

<sup>2</sup> Department of Hydrology & Water Resources Engineering, Shahid Chamran University of Ahvaz, Ahvaz, Iran

<sup>3</sup> Water Engineering Department, Urmia University, Urmia, Iran

<sup>4</sup> Institute of Research and Development, Duy Tan University, Danang 550000, Vietnam

<sup>5</sup> Faculty of Environmental and Chemical Engineering, Duy Tan University, Danang 550000, Vietnam

<sup>6</sup> Thuyloi University, 175 Tay Son, Dong Da, Hanoi, Vietnam

<sup>7</sup> Sustainable Management of Natural Resources and Environment Research Group, Faculty of Environment and Labour Safety, Ton Duc Thang University, Ho Chi Minh City, Vietnam